DOI: 10.17344/acsi.2023.8517 *Acta Chim. Slov.* **2024,** *71,* 186–196

Scientific paper

Extraction and Characterization of Nanocellulose from Waste of Date Palm "*Phoenix Dactylifera*" as Reinforcement of Polymer Composites

Meriem Kadri,[1] Nebia Bouzidi,[2,*] Toufik Chouana,[3] Hakim Belkhalfa,[4] Abdellah Henni[5] and Youcef Bouhadda[2]

[1] *Laboratory Research on Biological Systems and Geomatics, University Mustapha Stambouli of Mascara, Mascara 29000, Algeria*

[2] *Laboratory of Physical Chemistry of Macromolecules and Biological Interfaces, Faculty of Sciences, Department of Biology, University Mustapha Stambouli of Mascara, Mascara 29000, Algeria*

[2] *Laboratory for the protection of ecosystems in arid and semi-arid zones. University Kasdi Merbeh of Ouargla, Ouargla 30000 Algeria*

[4] *Scientific and Technical Research Center in Physicochemical Analysis, CRAPC, Bou-Ismail, Tipaza, Algeria*

[5] *Laboratory of Dynamic Interactions and Reactivity of Systems, University Kasdi Merbah of Ouargla, Ouargla 30000, Algeria*

** Corresponding author: E-mail: lina_kholoud@yahoo.fr*
Tel.: +213791182816

Received: 16-10-2023

Abstract

Cellulose is the most abundant and renewable polymer in nature. It is characterized by its biodegradability which helps create a friendly environment. This study seeks to describe the nanocellulose obtained from waste date palm, within the dried palms (DP) and the fresh palms (FP) through implementing chemical methods (hydrolysis with H_2SO_4). Physical properties, morphology, the elemental composition and the thermal stability were determined by Fourier transform infrared spectroscopy (FTIR), X-ray diffraction (XRD), zeta sizer, scanning electron microscopy (SEM), whereas energy dispersive X-ray (EDX) and thermogravimetric analysis (TGA), respectively. FTIR, SEM and EDX results revealed the effective removal of impurities, hemicellulose and lignin. After treatment, the dried palm (DR) samples contained 35.99% of cellulose and 33.12% of cellulose nanocrystals (CNC), while fresh palm (FP) samples 36.17% of cellulose and 34.35% of CNC. The CNCs have higher crystallinity than the raw fibers and Zeta sizer was between 25 and 1150 nm. TGA analysis showed that DP demonstrated noticeable thermal resistance.

Keywords: Nanocellulose; Date palm waste; Fibers; Extraction; Leaves of the date palm

1. Introduction

The depletion of fossil resources and the search for alternative solutions with an aim to secure the environment have stimulated interest towards the development of renewable and eco-friendly sustainable materials.[1–4]

Natural fiber composites, also known as natural fiber reinforced polymer composites have recently become highly valued materials. Aside from the expanding ecological, social, and economic awareness.[5] Natural fibers from residues and agricultural waste (e.g. flax, kenaf, hemp, sisal, jute) incorporated into these products either as fillers or reinforcement components within polymer matrices, opening avenues for diverse applications,[5,6] for example the paper industry, composites, biomedicine, textiles, construction, aerospace, automotive, to sensors, etc.[2]

Cellulosic fiber related to the main chemical constituent, cellulose, or lignocellulosic fibers, are amorphous matrices mostly composed of semi-crystalline cellulose microfibrils supported by hemicellulose, lignin, waxes, extractables and trace elements.[7–9] The materials based on cellulose, hemicelluloses and lignin, have several advantages for being renewable, biodegradable, and they do not

harm our environment. They are used to substitute petroleum materials.[10–12]

The cellulose is one of the most important natural resources. It is derived from plant cell walls and can be found in different sources like bacteria, algae, fungi, and some animals like tunicates.[13–17] Cellulose is found in the form of microfibril bundles oriented in various helical structures. Nanocrystalline celluloses (NCCs), or cellulose nanocrystals (CNCs) have generated a significant interest in the domain of materials science due to their intrinsic attractive properties, which include nanodimension, high surface area, high aspect ratio of 100, high crystallinity, low density, high mechanical strength, high dispensability in aqueous solutions, and unique morphology. Consequently, CNCs can be employed in various applications, such as reinforcement and support materials for nanocatalysts.[9,18–233, 5, 7, 9, 11, 13, and 15 m] In addition to films, hydrogels, and aerogels.[2]

Date palm (*Phoenix dactylifera*) belongs to the family *Plamae* (*Arecaceae*) and it is a tropical tree. The *Palmae* family comprises around 220 genera and about 2600 species.[24] It is the most significant agricultural crop, found abundantly in Northern. The date palm is an essential part of the flora of all Middle East and North Africa (MENA) countries. It plays a crucial role in the social, economic and cultural life of the region,[25] and it proves highly effective in the ongoing battle against desertification by providing a microclimate which prevents the long-term deterioration of ecologically fragile environments.[26,27] Furthermore, every tree lives for over than 100 years, yielding fruit and waste products, and large quantities of residues that are undoubtedly accumulated in agricultural lands, every year after date palm harvesting.[26–29] Each date palm tree generates about 30 kg of biomass with dry leaves contributing roughly 20 kg per year.[30] Waste is often disposed of by burning or in landfills, leading to significant environmental issues. Therefore, using specific natural fibers will not only minimize waste disposal challenges, but also environmental pollution.[5,6] The waste of date palm is interesting because of its abundance and relatively low cost in the manufacturing and industrial sector, in comparison to other vegetal fibers, which are currently used in the industrial fields.[6]

With the aim of the industrial exploitation this study investigates nanocellulose extracted from the leaves of the date palm tree (*Phoenix dactylifera* L). The leaves of the date palm were used as a source of cellulose in this work. We employed two types of waste materials, dried palm (DP) and fresh palm (FP), to examine the influence of maturation status on the properties of the extracted cellulose. Cellulose nanocrystals (CNCs) are derived from native cellulose by acid hydrolysis, which removes the amorphous parts. The resulting CNCs were characterized for their physicochemical, structural, morphological, and thermal properties to assess their potential as reinforcing materials in biocomposites.

2. Materials and Methods

2. 1. Plant Material

The samples of leaves (dry palm (DP) and fresh palm (FP)) of the date palm (*Phoenix dactylifera L*) were collected during the harvest period in their natural habit from Ouargla in the South-East of Algeria (31°54' to 32°1' North, 5°15' to 5°27' East).

2. 2. Chemical Reagents

Various chemical reagents were employed in the extraction and characterization process. These reagents included toluene, ethanol, sodium chlorite, acetic acid, sodium hydroxide, and sulfuric acid. All the chemicals were procured from Sigma-Aldrich.

2. 3. Chemical Compositions

The α-cellulose content, the acid-insoluble lignin and the ash content of specimens were determined according to the ASTMD 1103 – 55 T, ASTMD 1106-56 standard and ASTMD 1102-56 standard, respectively.[31]

2. 4. Isolation of Cellulose Fibers

The cellulose fibers were isolated as described by Mehany et *al.*[32] The palm residues were cleaned carefully three-four times under hot water to eliminate any dirt and other water-soluble compounds, and then dried in the open-air environment (between 25 and 30 °C). The residues were crushed then sieved a 60-mesh screen (250 µm) to cellulose fibers (Retch Control, model AS 200).

The extraction of cellulose was carried out following the methods outlined by Lu & Hsieh[33] Mellissa et *al.*[34] and Lu et *al.*[35] with some modifications (Figure 1):

10 g of palm powder were immersed in 150 ml of mixture of toluene and ethanol (2:1 v/v) for 20 hours. This step aimed to eliminate wax, pigments, and oils present in the palm powder. The resulting material from extraction was dried in an oven at 55 °C for 24 hours to remove any residual solvents and moisture. The dried palm powder was mixed with 10% NaOH solution (1 g/10 mL) at 75 °C for 1 hour. This treatment produced alkali-treated fibers by breaking down non-cellulosic components. The alkali-treated fibers, which constituted the insoluble pulps rich in cellulose, were subjected to a bleaching process. A 150 mL solution of 1% v/v sodium hypochlorite / deionized water, buffered to pH 5 using an acetate buffer, was used for bleaching. The mixture was stirred at 70 °C for 1 hour. The bleached fibers were washed at least three times with distilled water, or until the pH of the wash became neutral. Finally, the cellulose fibers were air-dried and weighed to obtain the final yield of extracted cellulose fibers.

2. 5. Isolation of Palm Nanocrystalline Cellulose

Isolation of palm nanocrystalline cellulose was performed using the method of Madureira et *al.* [36] with slight modification; the isolated cellulose was hydrolyzed with 64% wt sulfuric acid at an acid/cellulose ratio of 10 mL/g and at a temperature of 45 °C for 45 minutes. The acid hydrolysis was stopped by diluting with cold water (between 0 and 2 °C) for 10 times. The resulting cellulose nanocrystal gel was washed twice, centrifuged (Hettich Rotina, model 380R) at 5000 rpm for 30 min at 10 °C, and then dialyzed with regenerated cellulose dialysis membranes with a molecular weight cutoff of 12–14 KDa, against ultrapure water for 4 days and until neutral pH was achieved. The suspension was sonicated (53Church Hill Newtown, model VC505) in an ice bath for 30 min, then frozen at –30 °C, and freeze-dried. The dried product was stored for subsequent characterizations. The values were determined in triplicate.

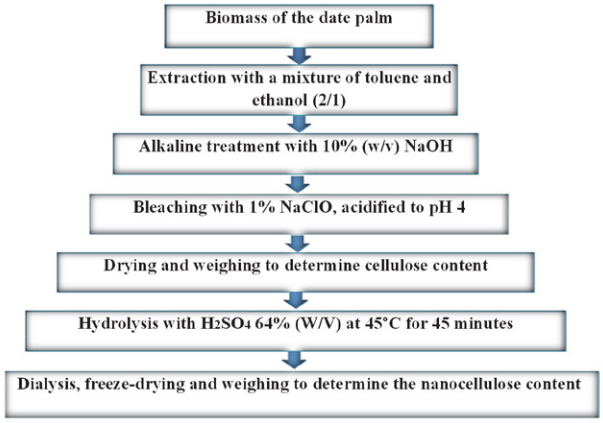

Figure1. The extraction process of nanocellulose from palm fibers

2. 6. Characterization of Nanocellulose

Fourier Transform Infrared (FTIR)

Infrared spectroscopy was performed using an FTIR spectrometer (Cary 660 FTIR). The measurements were conducted in the range of 4000–400 cm^{-1} with a resolution of 8 cm^{-1}

X-ray diffraction (XRD)

XRD measurements were carried out using a Proto Benchtop XRD instrument under room conditions. The analysis was performed at 2θ ranging from 5° to 40° with a step of 0.02° and a scan rate of 2 s/step. XRD analysis provides information about the crystalline structure of the nanocellulose.

Crystalline Index (CrI) values were calculated using two equations (Eq 1 and Eq 2).[37,38]

$$CrI = [(I_{max} - I_{am})/ I_{max}] \text{ X } 100 \quad (1)$$

$$CrI = (A_{Cry} / A_{Total}) \text{ X } 100\% \quad (2)$$

where I_{max} is the peak intensity at the crystalline plane (2θ = 22.6°), and I_{am} is the minimum intensity located between the two most distinct peaks (2θ = 18.7°). A_{Cry} is the sum of crystalline band areas, and A_{Total} is the total area under the diffractograms. The calculated crystallinity index provides a measure of the degree of crystallinity in the nanocellulose sample.

The crystal size (D) of the nanocellulose was estimated using the following equation (Eq 3).

$$D = (K \lambda) / \beta \cos\theta \quad (3)$$

where K is the Scherrer constant, λ is the wavelength of X-ray radiation, β is the full width at half maximum (FWHM) of the peak, and θ is the diffraction angle.

Thermogravimetric analysis (TGA)

The thermal stability of the cellulose nanocrystals (CNCs) was analyzed using a TGA instrument (differential thermogravimetry) –51H. The specimens were heated from room temperature to 700 °C at a heating rate of 10 °C/min under a N_2 gas flow rate of 60 mL/min.

Scanning electron microscopy (SEM)

The microstructural analysis of the raw fibers and CNCs of palm fibers was carried using the scanning electron microscope (EVO15, smart EDX Zeiss). The dried sample powder was placed on carbon strips and coated with a thin gold layer under an argon atmosphere. Micrographs were taken at an accelerating voltage of 15 kV.

Zeta sizer

The suspensions of CNCs (0.05% w/v) were examined using a Zetasizer HORIBA Scientific SZ-100 for zeta size analysis.

3. Results and Discussion

3. 1. Isolation and Purification of Cellulose

The chemical compositions of the fibers obtained before the purification is shown in table 1. These results are consistent with findings from other researchers.

The obtained results showed that the cellulose is the most chemical constituent of date palm fibers. The cellulose was isolated from palm fibers with an interesting rate of 35.99% ± 2.64 for DP and 36.17% ± 0.66 for FP. According to Astruc et *al.*[39] the cellulose yield of the fibers, the level of polymerization of the cellulose and the angle of the

spirals in each wall vary for each plant and have a direct influence on their physical and chemical properties**.**

The standard deviations associated with the cellulose yield percentages indicate possible measurement errors. However, these values obtained through the purification process demonstrate its effectiveness in isolating cellulose from palm fibers. Additionally, the chemical compositions of the fibers before the purification processes were consistent with previous research, confirming the reliability of the obtained results. Further analysis and characterization of the isolated cellulose will provide more insights into its properties, allowing for a comprehensive understanding of its potential applications in various fields.

Table 1. Chemical compositions of different palm fibers

Component	Present work		Sbiai et *al.* (2010)[40]	Gouamid (2015)[41]	Jonoobi et *al.* (2019)[28]
	DP	FP			
Cellulose (%)	35.99	36.17	54.75	38.10	40.21
Lignin (%)	18.07	16.45	15.30	11.95	32.2
Extractible (%)	20.16	24.10	8.2	19.46	4.24
Ashes (%)	8.21	8.78	1.75	7.75	10.54
Moisture (%)	4.89	4.21	/	/	/
Hemicellulose(%)	/	/	/	22.7	12.8

Alkaline dilute treatment was used to mainly dissolve lignin, pectin, hemicelluloses and proteins. Furthermore, a bleaching step was carried out to eliminate any remaining lignin residues.[42]

The isolation and purification of cellulose from palm fibers followed a three-step procedure consisting of dewaxing, delignification, and hemicellulose elimination. Each step contributed to transforming palm fiber into a clean white color. The physical appearance of palm fibers before and after purification is illustrated in Figure 2(d). The palm fibers appear as white cottony fibers, after alkali and bleaching process. The change in color indicates the effective removal of a significant amount of non-cellulosic components during the purification process.

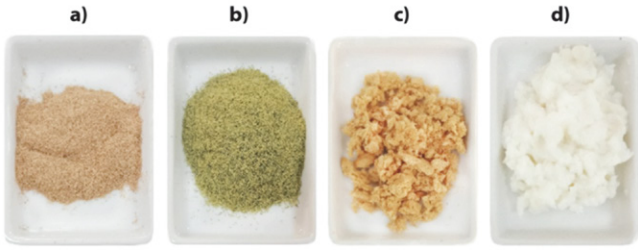

Figure 2. Raw fibers of DP (a), raw fibers of FP (b), delignified fibers (c) and bleached fibers (d)

3. 2. Preparation of the Cellulose Nanocrystals

The purified cellulose was further treated by sulfuric acid hydrolysis in the following conditions: 45°C, 45 min and 64% (wt) H_2SO_4 concentration. These conditions were determined based on research by several authors,[33,36,43,44] who emphasized the critical role of acid concentration, hydrolysis temperature, and time as crucial parameters in CNCs isolation.

According to Lu et *al.*[35] the yield of CNCs by sulfuric hydrolysis ranged from 10% to 80%. The yield of CNCs in this work is in this range with 33.12% ± 2.51 for DP and 34.35% ± 0.18 for FP.

The yield is attributed to the additional hydrolysis of the amorphous regions of the cellulose, according to Nang et *al.*[45] Acid hydrolysis is a widely utilized method for manufacturing nanocrystalline cellulose (NC). It proves to be effective due to its ability to selectively degrade the amorphous regions of cellulose microfibrils, while preserving the crystalline domains. Consequently, these preserved crystalline domains can be isolated and obtained as monocrystals. In general, there are numerous factors that influence the yield, not just the reaction conditions like the acid type and concentration, the time of hydrolysis and temperature, also the mechanic treatments, the centrifugation throughout the procedure and fibers characteristics.[35]

3. 3. Fourier Transform Infrared (FTIR)

The Fourier transform infrared (FTIR) analysis provided valuable information about the chemical changes that occurred during the purification and isolation of cellulose nanocrystals (CNCs). Figure 3 shows the comparison of the FTIR spectra of various stages of the process, including raw fibers, dewaxed fibers, delignified cellulose, and CNC.

The presence of a peak at 2849 cm^{-1} in the FTIR spectrum of raw fibers, attributed to waxes, indicates the presence of extractable materials in the initial fibers. However, after the dewaxing step, this peak is absent, confirming the effective removal of waxes and other extractables from the fibers.

Regarding lignin, characteristic peaks were observed in the FTIR spectra of raw fibers, including peaks at 1516 cm^{-1} (aromatic backbone vibration), 1508 cm^{-1} (C=C vibrations of aromatic rings), and 1243 cm^{-1} (C-O bonds of carboxylic and ether groups). These peaks are

indicative of the presence of lignin. However, after the delignification stage, these peaks diminish or disappear completely, indicating the successful elimination of lignin from the cellulose structure. The presence of specific peaks at 1230 cm^{-1}, 1461 cm^{-1}, and 1517 cm^{-1} in the FTIR spectra confirms the complete sequential removal of lignin during the purification process. These results align with previous studies by Astruc et *al.*[3] and demonstrate the effectiveness of the purification steps in eliminating lignin from the cellulose fibers. Generally speaking, the FTIR analysis provides strong evidence of the successful purification of cellulose and the removal of waxes and lignin, validating the purity of the obtained cellulose and its suitability for further processing into cellulose nanocrystals.

The presence of characteristic peaks at 1729 cm^{-1} and 1700 cm^{-1} in the FTIR spectrum indicates the presence of carbonyl stretching vibrations, which are attributed to hemicelluloses.[33,36] Additionally, the peak at 1700 cm^{-1} is associated with acetyl and ester groups in hemicellulose, or carboxylic acid groups.[35] The disappearance of these peaks in the FTIR spectra of delignified cellulose and CNCs indicates the successful removal of hemicellulose from the palm fibers. The purification process effectively eliminates hemicellulose, resulting in the isolation of cellulose-rich materials. The removal of hemicellulose is crucial for obtaining purified cellulose materials since hemicellulose contributes to the amorphous regions of the fibers and can affect the properties of the final product. By eliminating hemicellulose, the delignified cellulose and CNCs obtained have a higher cellulose content and enhanced crystallinity, making them suitable for reinforcement application.

The band observed in the range of 3400–3000 cm^{-1} corresponds to the stretching vibrations of hydroxyl groups (-OH) present in cellulose, as noted by Astruc et *al.*[43] The FTIR spectra of cellulose typically exhibit several distinct bands that can be attributed to specific functional groups within the cellulose structure. These include the stretching of OH bonds at 3362 cm^{-1}, the asymmetric angular deformation of C-H bonds at 1429 cm^{-1}. The symmetric angular deformation of C-H bonds at 1371 cm^{-1}.The stretching of C-OH and C-C-OH bonds in secondary and primary alcohols at 1110 cm^{-1} and 1059 cm^{-1}, respectively, and the angular deformation of C-H bonds at 897 cm^{-1}, as reported by Vasconcelos et *al.*[46] Additionally, Madureira et *al.*[36] identified peaks at 3310 cm^{-1} and 1640 cm^{-1}, respectively, associated with cellulose, as well as a peak at 2900 cm^{-1} attributed to C-H stretching vibrations, which are present in all samples.

The presence of peaks at 3400–3000 cm^{-1}, 2900 cm^{-1}, 1110.9 cm^{-1}, 1059 cm^{-1}, and 897 cm^{-1} in the FTIR spectrum (as shown in figure 3) confirms the presence of cellulose throughout the purification and extraction processes of CNCs. These results indicate that cellulose is retained and not eliminated during the purification and extraction steps; supporting the successful isolation of CNCs while maintaining the cellulose structure.

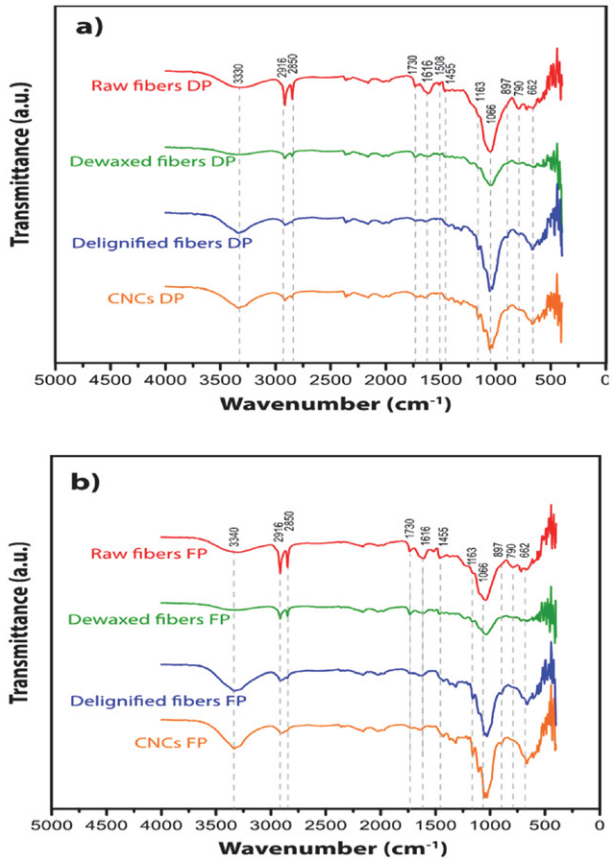

Figure 3. FTIR spectroscopy of DP (a) and FP (b) at different stage of treatment

3. 4. X-ray Diffraction (XRD)

The crystallinity of nanocellulose is a main factor in determining its thermal stability and mechanical properties.[47] The crystallinity study allows to determine the effect of extraction methods on the crystal structure of the cellulose. X-ray diffraction (XRD) technique was utilized to identify the CrI of raw fibers and nanocrystals (Figure 4).

Studies by Culsum et *al.*[23] and Lu et *al.*[35] report that the characteristic diffraction peaks of cellulose appear at $2\theta \approx 15.71$, 16.48 and 22.50, representing different crystallographic planes. Similarly, the XRD patterns of bacterial cellulose from Vasconcelos et *al.*[46] align with these characteristic peaks.

As shown in figure 4, the XRD patterns of the samples also reveal these characteristic diffraction peaks of cellulose at 2θ values of approximately 15, 17, and 22°. Additionally, a distinct peak at $2\theta \approx 22$ indicates the presence of a crystalline region.

Table 2 provides the measured values for the crystallinity index (%), and crystallite size obtained from X-ray

diffraction curves. The CNCs fibers exhibited the highest crystallinity index value, while the lowest value was observed for the raw fibers. These results are well correlated with values of Rajinipriya et *al.*[2] Dahlem et *al.*[48] and Gond et *al.*[49]

Dahlem et *al.*[48] reported that the raw fibers had a crystallinity index of 40.62%, while the CNC exhibited a higher value of 66.19%. Similarly, Gond et *al.*[49] found that the raw fibers had a crystallinity index of 32.4%, whereas the CNC showed a higher value of 53.02%. Both studies concluded that the crystallinity of the nanocellulose (NC) was higher compared to that of the initial material. This increase in crystallinity can be attributed to the application of a chemical treatment, which effectively eliminated the non-cellulosic components of the fibers.

According to Vasconcelos et *al.*[46] the increasing crystallinity following the acid hydrolysis reaction is a result of a decrease in amorphous content, because this region is more available to acid attack.

The obtained crystallite size values are in close agreement with those reported by Gondet*al.*[49] who found a size of 3.74 nm for raw fibers and 3.4 nm for CNC.

A number of parameters such as the source of cellulose, isolation process conditions and various pretreatments determine the final crystallinity of nanocellulose in either crystal or fiber form.[50]

Biomass of lignocellulosic components consists of amorphous and crystalline regions. The amorphous region is mainly due to lignin and hemicellulose, while the crystalline region is attributed cellulose. Therefore, the treatment that is done chemically leads to the depolymerization of hemicellulose and the delignification of fibers, which tends to increase the crystallinity of cellulose obtained.[51]

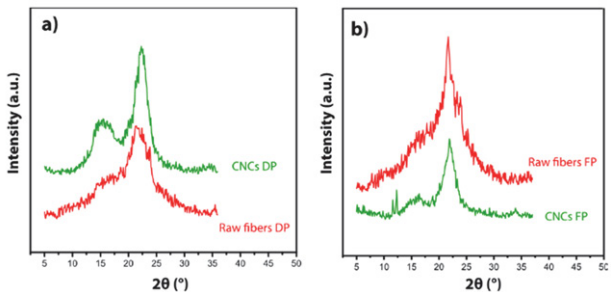

Figure 4.DRX of DP (a) and FP (b)

Table 2. The results of crystallinity index and crystal size of studied raw fibers and CNC

	Crystallinity index (%)	Crystal size (nm)
Raw fibers DP	35.09	5.85
CNCs DP	53.34	3.03
Raw fibers FP	28.0	5.53
CNCs FP	57.7	3.48

3. 5. Zeta Sizer

Particle size measurement using a Zetasizer or Nanosizer is commonly used to determine the size distribution and assess the dispersion and stability of CNCs in aqueous solutions.[20,23] The analysis provides information on the size range and distribution of the particles. In the Figure 5, it is evident that the size of CNC particles obtained from DP ranges from 25 to 1000 nm with an average of 512.5 nm. In contrast, for CNC particles obtained from FP, the size range is 76 to 1150 nm, with an average of 613 nm. These findings are consistent with previous studies that have reported CNC sizes ranging from 5.6 to 1106 nm; 30 nm to 1 µm.[43]

The broad distribution observed can be attributed to the anisotropic properties of the CNC suspension in solution.[43] It is important to note that the size distribution obtained from light diffusion techniques like the Zeta sizer may not provide precise and accurate measurements of particle size, as it measures the length and diameter of particles. However, the results can still provide valuable information about the general size range and distribution of the CNC particles. For more detailed and accurate information about the particle size and morphology of CNCs, microscopy techniques are recommended. The size distribution obtained from the Zeta sizer analysis often aligns well with the results obtained by microscopy, further confirming the overall size range and distribution of CNC particles.

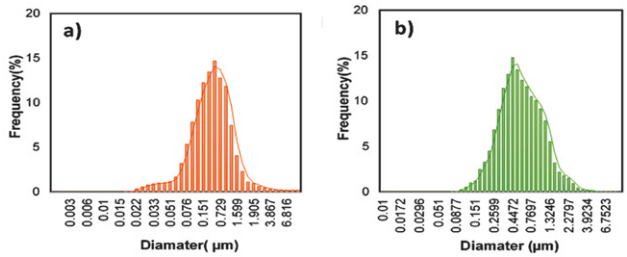

Figure 5. Zeta sizer of CNCs-DP (a) and CNCs-FP (b)

3. 6. Scanning Electron Microscopy (SEM) Analysis

SEM images (figure 6) provide valuable insights into the surface morphologies of palm fibers before and after chemical treatments. The untreated palm fibers (Figure 6 a1 and b1) appear as large bundles with rough surfaces. The presence of wax, oil, and surface impurities is clearly visible, indicating the presence of cellulose fibers embedded in hemicelluloses and lignin. These substances are effectively removed during the delignification process, as shown in Figure 6 (a2 and b2), resulting in a more defined and shorter cellulose fiber size with an approximate diameter of 4.98 µm.

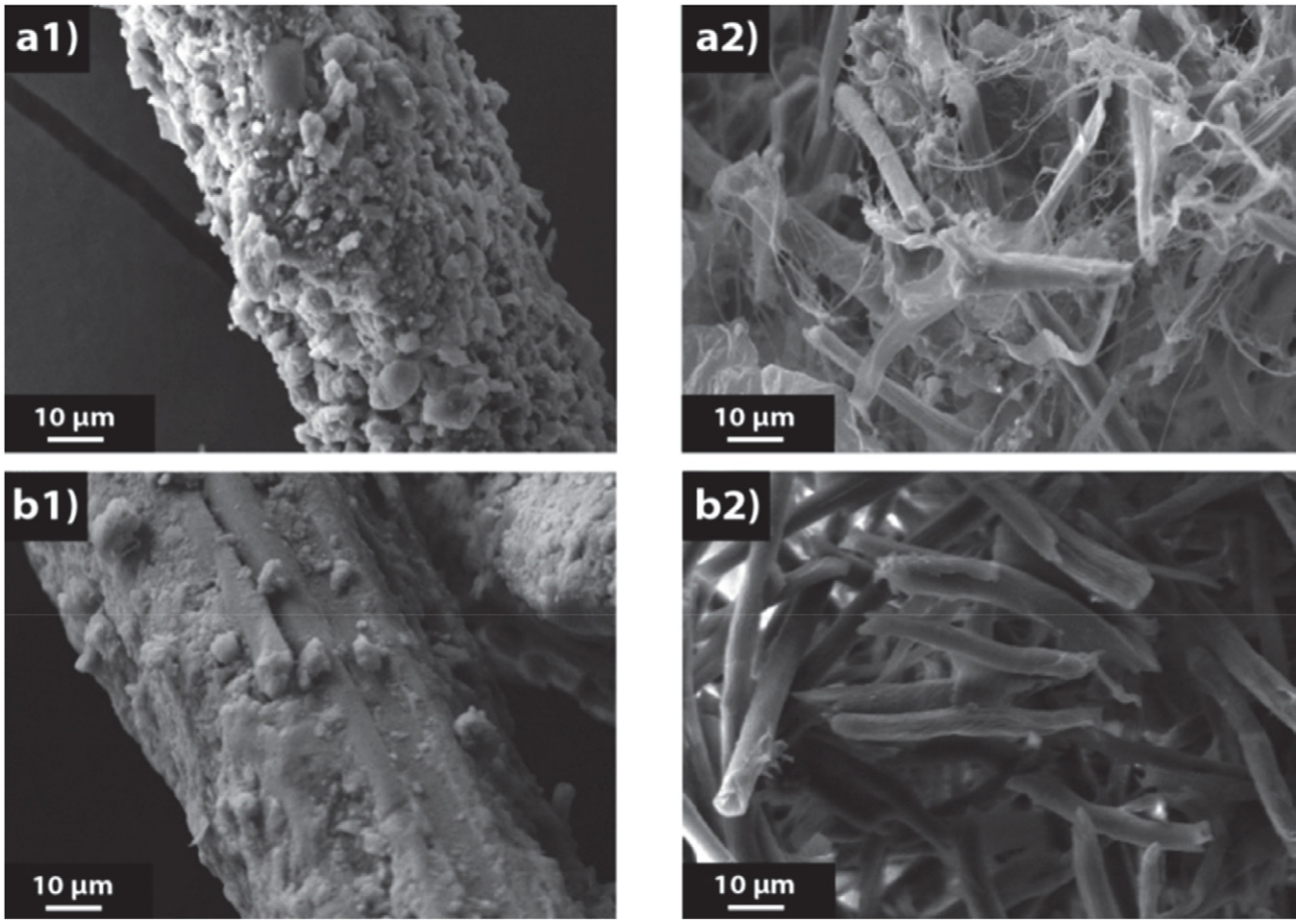

Figure 6. SEM micrographs of raw fibers of DP (a1), CNCs-DP (a2), raw fibers of FP (b1) and CNCs-FP (b2)

According to Ali et *al.*[52] alkaline and acid treatments of cellulosic fibers generally result in a more transparent, clearer, and harder surface with dispersed fibers compared to the raw form. in this study, the sulfuric acid treatment (64%) effectively disintegrates the palm fibers, reducing their size to nanocrystalline cellulose.

The presence of wax, oil, and impurities on the surface of untreated fibers is clearly observed. The treated fiber clusters, shown in Figure 6, exhibit a smoother surface, indicating the removal of hemicelluloses, lignin, wax, oils, and other impurities. This improvement in surface morphology is consistent with the results reported by Zarina and Ahmed.[53]

Overall, SEM analysis reveals the morphological changes that occur after the chemical treatments, confirming the removal of impurities and the transformation of palm fibers into nanocrystalline cellulose with improved surface characteristics.

3. 7. Energy Dispersive X-ray Spectroscopy (EDX)

The EDX spectrum shows the spectra peaks that correspond to the binding energies of carbon, oxygen and other elements as the major components. The EDX spectrum reveals the presence of trace elements and impurities in the treated cellulose material. This is not unusual and can be influenced by various factors, including the source of the cellulose, the purification process, and the specific treatment methods employed. The detection of calcium (Ca), chlorine (Cl), and silicon (Si) as impurities indicates the presence of these elements in the treated cellulose. These impurities could arise from the raw material itself, such as minerals present in the plant fibers used for cellulose extraction. They can also originate from the processing methods used, including the chemicals and equipment employed during the treatment process. The presence of these trace elements does not necessarily indicate a negative aspect, but their quantities should be evaluated to ensure they are within acceptable limits for the intended applications of the cellulose material. The presence of residual sulfur (S) in small amounts can be attributed to the H_2SO_4 acid hydrolysis process used for the extraction of cellulose nanocrystal (CNC). The sulfuric acid used in the hydrolysis process can leave residual traces in the final CNC product. While efforts are made to minimize residual impurities during purification and extraction processes, the detection of sulfur suggests that some residual

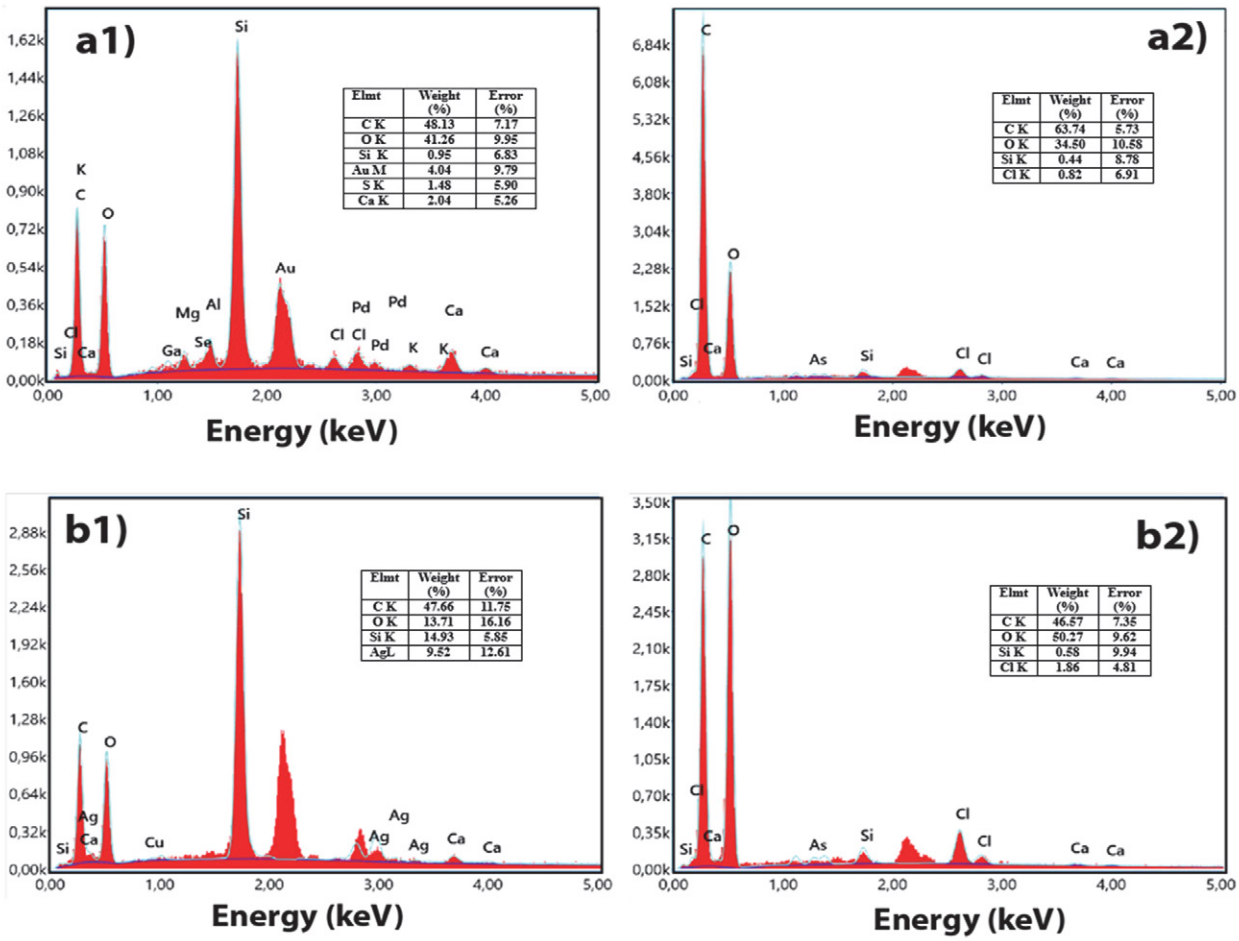

Figure 7. EDX of raw fibers of DP (a1), CNCs-DP (a2), raw fibers of FP (b1) and CNCs-FP (b2)

impurities from the acid treatment remain. These residual impurities should be considered when evaluating the purity and suitability of the CNC for specific applications. It's worth noting that the EDX spectrum provides qualitative elemental analysis, indicating the presence of different elements in the sample. For more accurate quantification of these elements, additional analytical techniques such as atomic absorption spectroscopy or inductively coupled plasma mass spectrometry may be employed. It's worth mentioning that in the raw fibers, elements such as calcium (Ca), silicon (Si), chlorine (Cl), magnesium (Mg), and potassium (K) are also present. These elements may be naturally present in the palm fibers or could be introduced during the growth or processing stages. The EDX analysis provides valuable information about the elemental composition and impurities present in the cellulose samples, confirming the effectiveness of the treatment in removing certain impurities while also indicating the residual presence of some elements originating from the extraction process.

Considering both the natural presence of certain elements in the raw fibers and the residual elements from the extraction process, it is important to determine the acceptable limits for these impurities based on the specific applications of the cellulose material. Quality control measures and appropriate purification techniques can help ensure that the final cellulose product meets the required standards for its intended use. These results and observations are in accordance with the results carried out by Ali et *al.*[52]

3. 7. Thermogravimetric Analysis (TGA)

The thermogravimetric analysis allows for measurement of the degradation of a sample according to the temperature end /or time.[54] Concerning the thermogravimetric analysis of the date palm fibers, results are illustrated in figure 8.

The initial weight decrease observed in the TGA measurement of CNCs in the range of 25–220 °C is likely due to the evaporation of water absorbed on the surface of CNCs. The subsequent weight loss observed between 220 °C to 360 °C can be attributed to the breaking or rearranging the glycosidic bonds of the CNCs, leading to cellulose degradation processes such as depolymerization, dehydration, and decomposition of glycosyl unit.[23]

Our results (Table 3) reveal that date fibers show two distinct degradation peaks with confirm the results reported by Bourmaude*t al.*[30] who reported that the date palm

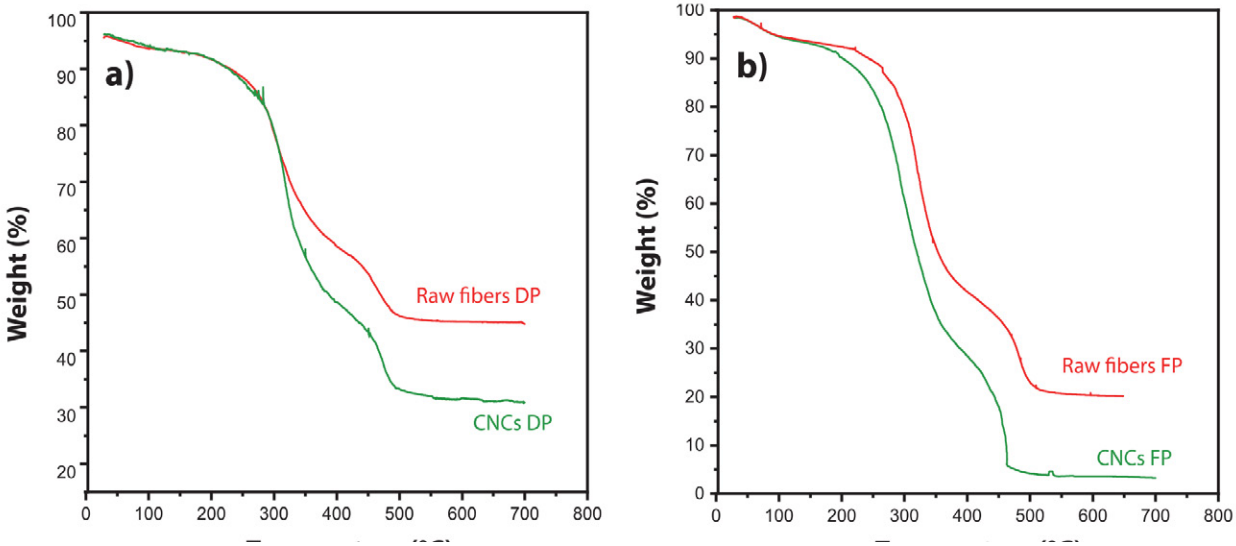

Figure 8. TGA of DP (a) and FP (b)

fibers have better thermal stability compared to other natural fibers.

According to Ali et *al.*[52] the thermal degradation of cellulose generally occurs in three phases. The initial weight losses for the samples were due to the evaporation of absorbed or surface-bound moisture (H_2O), which was evaporated below 100 °C. The degradation of CNC began at 259 °C, with the onset and offset temperatures for cellulose degradation occurring between 277 °C and 387 °C as measured by TGA.

The thermal degradation behavior of the samples can be further explored by referring to Table 3, which presents the specific onset and offset temperatures associated with weight loss and the degradation of the cellulose material.

Figure 8 and Table 3 clearly demonstrate that the CNC-DP exhibits significantly higher thermal stability compared to CNC-FP, with a weight loss of 14.74% for DP and 30.67% for FP. The disparity in thermal stability can be attributed to differences in the size, structure, and surface properties of the CNCs.

In terms of the thermal stability of the chemical components present in lignocellulosic materials, Raju et *al.*[9] indicate that hemicellulose, lignin, and cellulose exhibit different levels of thermal stability. Generally, hemicellulose is less thermally stable compared to lignin and cellulose. In the case of treated fibers, the removal of impurities, such as lignin and hemicellulose, during the chemical treatment process can lead to an improvement in thermal stability compared to untreated fibers. These findings highlight the influence of chemical treatments on the thermal stability of cellulose and lignocellulosic materials, with the potential to improve their thermal properties and expand their application possibilities

4. Conclusion

This study explored the potential of the date palm (*Phoenix dactylifera L*) waste leaves as a source of nanocellulose (CNC) with tailorable properties. Agricultural wastes represent an immense source of natural fibers, and utilizing them for CNC production offers a sustainable and cost-effective approach. In order to study the influence of the degree of maturity on the properties of the extracted nanocellulose, two types of waste material were used, that is dried palm (DP) and fresh palm (FP).

Alkaline and bleaching treatments effectively removed lignin, hemicellulose and impurities, as confirmed by FTIR and SEM micrographs. While EDX revealed traces of chemical impurities on the treated nanocellulose. XRD analysis revealed a higher degree of crystallinity for the CNCs compared to the raw fibers. Zeta sizer results

Table 3. The thermal degradation of studied raw fibers and CNCs

Samples	1st thermal degradation			2nd thermal degradation			Char yield
	T Onset (°C)	T Offset (°C)	WL (%)	T Onset (°C)	T Offset (°C)	WL (%)	(%)
Raw fibers DP	266.91	372.13	25.32	423.87	493.00	10.13	**15.19**
CNC DP	263.17	349.91	28.01	421.72	495.01	13.27	**14.74**
Raw fibers FP	265.22	375.99	43.26	451.28	511.93	14.35	**28.91**
CNC FP	226.61	353.50	51.24	414.65	464.82	20.57	**30.67**

showed that the size ranging was between 25 and 1150 nm. The TGA showed a high thermal stability for DP compared with FP.

Based on the findings, comparatively, more mature date palm leaves (DP) demonstrate slightly superior characteristics especially in terms of crystallinity and thermal stability when compared to fresher palm leaves (FP). This suggests that the degree of maturity can influence the final properties on the CNCs. The study emphasizes the significance of particle characteristics, including crystallinity, size, as well as the thermal stability of CNC particles, coupled with the low cost and abundant availability of the source material, date palm CNC emerges as an appealing option for reinforcing polymer materials.

5. References

1. H. Kargarzadeh, M. Ioelovich, I. Ahmad, S. Thomas, A. Dufresne, Handbook of Nano-cellulose and Cellulose Nanocomposites, Wiley-VCH, Verlag. **2017**, 23. **DOI:**10.1002/9783527689972
2. M. Rajinipriya, M. Nagalakshmaiah, M. Robert, S. Elkoun, *ACS Sustain. Chem. Eng.* **2018**, *6*, 2807–2828. **DOI:**10.1021/acssuschemeng.7b03437
3. J. Astruc, M. Grandbois, G. Laroche, M. Robert, S. Elkoun, *Can. J. Chem*. **2021**, *99*, 1–25. **DOI:**10.1139/cjc-2020-0371
4. K. J. Nagarajan, N. R. Ramanujam, M. R. Sanjay, S. Siengchin, B. Surya Rajan, K. SathickBasha, P. Madhu, G. R. Raghav, *Polym. Compos*. **2021**, *42*, 1588–1630. **DOI:**10.1002/pc.25929
5. F. M. Al-Oqla, S. M. Sapuan, *J. Clean. Prod.* **2014**, *66*, 347–354. **DOI:**10.1016/j.jclepro.2013.10.050
6. B. Chihaoui, F. S. Parareda, Q. Tarrés, F. X. Espinach, S. Boufi, M. Delgado-Aguilar, *Polym*. **2020**, *18*, 1693. **DOI:**10.3390/polym12081693
7. S. Azizi, F. Alloin, A. Dufresne, *Biomacromolecules* **2005**, *6*, 612–626. **DOI:**10.1021/bm0493685
8. Y. Habibi, L. A. Lucia, O. J. Rojas, *Chem. Rev*. **2010**, *110*, 3479–3500. **DOI:**10.1021/cr900339w
9. V. Raju, R. Revathiswaran, K. S. Subramanian, K. T. Parthiban, K. Chandrakumar, E. V. Anoop, C. J. Chirayil, *Sci. Rep*. **2023**, *13*, 1199. **DOI:**10.1038/s41598-022-26600-5
10. A. Dufresne, *Mater. Today* **2013**, *16*, 220–227. **DOI:**10.1016/j.mattod.2013.06.004
11. B. Thomas, M. C. Raj, B. K. Athira, H. M. Rubiyah, J. Joy, A. Moores, G. L. Drisko, C. Sanchez, *Chem. Rev.* **2018**, *118*, 11575–11625. **DOI:**10.1021/acs.chemrev.7b00627
12. C. R. Contessa, G. S. Da Rosa, C. C. Moraes, *Int. J. Mol. Sci.* **2021**, *22*, 10628. **DOI:**10.3390/ijms221910628
13. H. Ng, L. T. Sin, T. Tee, S. Bee, D. Hui, C. Low, A. R. Rahmat, *Compos. B* **2015**, *75*, 176–200. **DOI:**10.1016/j.compositesb.2015.01.008
14. N. Kanai, T. Honda, N. Yoshihara, T. Oyama, *Cellulose* **2020**, *27*, 5017–5028. **DOI:**10.1007/s10570-020-03113-w
15. L. Y. Ng, T. J. Wong, C. Y. Ng, C. K. M. Amelia, *Arab. J. Chem.* **2021**, *14*, 10339. **DOI:**10.1016/j.arabjc.2021.103339
16. D. K. Arserim-Uçar, F. Korel, L. S. Liu, K. L. Yam, *Food Chem.* **2021**, *336*, 127597. **DOI:**10.1016/j.foodchem.2020.127597
17. N.E.A. El-Naggar, A.B.A. Mohammed, S.E. El-Malkey, *Sci. Rep*. **2023**, *12*, 18533. **DOI:**10.1038/s41598-022-26642-9
18. M. R. Ishak, S. M. Sapuan, Z. Leman, M. Z. A. Rahman, U. M. K. Anwar, *J. Therm. Anal. Calorim*. **2012**, *109*, 981–989. **DOI:**10.1007/s10973-011-1785-1
19. S. Mondal, *Carbohydr. Polym*. **2017**, *163*, 301–316. **DOI:**10.1016/j.carbpol.2016.12.050
20. R. A. Ilyas, S. M. Sapuan, M. R. Ishak, *Carbohydr. Polym.* **2018**, *181*, 1038–1051. **DOI:**10.1016/j.carbpol.2017.11.045
21. J. H. Jordan, M. W. Easson, B. Dien, S. Thompson, B. D. Condon, *Cellulose* **2019**, *26*, 5959–5979. **DOI:**10.1007/s10570-019-02533-7
22. I. Uddin, S. Thomas, R. K. Mishra, A. M. Asiri (Ed.) : Sustainable polymer composites and nanocomposites, Springer, **2019**, pp. 37–65. https://link.springer.com/book/10.-1007/978-3-030-05399-4
23. N. T. U. Culsum, C. Melinda, I. Leman, A. Wibowo, Y. W. Budhi, *Mater. Today Commun.* **2021**, *26*, 101817. **DOI:**10.1016/j.mtcomm.2020.101817
24. A. Faiad, M. Alsmari, M. M. Z. Ahmed, M. L. Bouazizi, B. Alzahrani, H. Alrobei, *Sustain*. **2022**, *14*, 1134. **DOI:**10.3390/su14031134
25. R. A. Nasser, H. A. Al-Mefarrej, *World Appl. Sci. J.* **2011**, *15*, 1651–1658
26. A. Bendahou, H. Kaddami, M. Raihane, Y. Habibi, A. Dufresne, *Rev. Roum. Chim*. **2009**, *54*, 571–575.
27. W. Ghori, N. Saba, M. Jawaid, M. Asim, *IOP Conf. Mater. Sci. Eng.* **2018**, *368*, 012009. **DOI:**10.1088/1757-899X/368/1/012009
28. M. Jonoobi, M. S. H. *J. Renew. Mater.* **2019,** *7*, 1055–1069. **DOI:**10.32604/jrm.2019.08188
29. S. Awad, Y. Zhou, E. Katsou, Y. Li, M. Fan, *Waste Biomass Valori* **2020**, *12*, 2853–2887. **DOI:**10.1007/s12649-020-01105-2
30. A. Bourmaud, H. Dhakal, A. Habrant, J. Padovani, D. Siniscalco, M. H. Ramage, J. Beaugrand, D. U. Shah, *Comps. A: Appl. Sci. Manuf.* **2017**,*103*, 292–303. **DOI:**10.1016/j.compositesa.2017.10.017
31. American Society, "ASTM Standards On Wood, Wood Preservatives, And Related Materials" **1959**, 139–150. http://archive.org/details/astmstandardsonw00amer
32. S. Mehanny, E. E. Abu-El Magd, M. Ibrahim, M. Farag, R. Gil-San-Millan, J. Navarro, A. E. H. El Habbak, E. El-Kashif, *J. Mater. Res. Technol.* **2021**, *10*, 526–537. **DOI:**10.1016/j.jmrt.2020.12.027
33. P. Lu, Y. L. O. Hsieh, *Carbohydr. Polym.* **2012**, *81*, 564–573. **DOI:**10.1016-/j.carbpol.2011.08.022
34. B. A. Melissa, S. M. M .A. Bashir Ahmmad, *J. Reinf. Plast. Compos.* **2014**, *33*, 2205–2213. **DOI:**10.1177/0731684414558325
35. S. Lu, T. Ma, X. Hu, J. Zhao, X. Liao, Y. Song, X. Hu, *J. Sci. Food Agric.* **2022**, *102*, 312–321. **DOI:**10.1002/jsfa.11360
36. A. R. Madureira, T. Atatoprak, D. Çabuk, F. Sousa, R. C. Pul-

lar, M. Pintado, *Int. J. Food Stud.* **2018**, *7*, 24–33. **DOI:**10.7455/ijfs/7.1.2018.a3
37. L. Segal, J. J. Creely, A. E. Martin, C. M. Conrad, *Text. Res. J.* **1959**, *29*, 786–794. **DOI:**10.1177/004051755902901003
38. H. Hermans, J. J. Hermans, A. Weidinger, *J. Polym. Sci.* **1948**, *169*, 1–9. **DOI:**10.1002/pol.1948.120030101
39. J. Astruc. Extraction et compatibilisation de nanocristaux de cellulose issue de résidus lignocellulosiques pour le renforcement de biocomposites, Québec, Canada, **2018**, 1–150. https://core.ac.uk/download/pdf/199228206.pdf
40. A. Sbiai, A. Maazouz, E. Fleury, H. Sautereau, H. Kaddami, *Bioresources* **2010**, *5*, 672–689. **DOI:**10.15376/biores.5.2.672-689
41. M. Gouamid, Contribution of the study of diagnosis and valuation of El ghars palm waste, Ouargla, Algeria, **2015.** https://search.mandumah.com/Record/944117
42. W. P. F. Netoa, H. A. Silvérioa, N. O. Dantasb, D. Pasquini, *Biomass. Bioenerg.* **2012**, *46*, 555–563. **DOI:**10.1016/j.biombioe.2012.06.039
43. J. Astruc, M. Nagalakshmaiah, G. Laroche, M. Grandbois, S. Elkoun, M. Robert, *Carbohydr. Polym*. **2017**, *178*, 352–359. **DOI:**10.1016/j.carbpol.2017.08.138
44. T. Gabriel, A. Belete, G. Hause, R. H. H. Neubert, T. Gebre-Mariam, *J. Polym. Environ*. **2021**, *29*, 2964–2977. **DOI:**10.1007/s10924-021-02089-3
45. N. An, H. T. Chi Nhan, T. D. Tap, T. T. T.Van, V. P. Van , L. Van Hieu, *J. Polym. Environ*. **2020**, *28*, 1465–1474. **DOI:**10.1007/s10924-020-01695-x
46. N. F. Vasconcelos, J. P. A. Feitosa, F. M. P. da Gama, J. P. S. Morais, F. K. Andrade M. S. M. de Souza Filho, M. F. Rosa, *Carbohydr. Polym.* **2017**, *155*, 425–431. **DOI:**10.1016/j.carbpol.2016.08.090
47. E. Dinçel Kasapoğlu, S. Kahraman, F. Tornuk, *Foods* **2023**, *12*, 746. **DOI:**10.3390/foods12040746
48. M. A. Dahlem, C. Borsoi, B. Hansen, A. L. Catto, *Carbohydr. Polym*. **2019**, *218*, 78–76. **DOI:**10.1016/j.carbpol.2019.04.064
49. R. K. Gond, M. K. Gupta, M. Jawaid, *Polym. Compos.* **2021**, *42*, 5400–5412. **DOI:**10.1002/pc.26232
50. M. Jonoobi, *Cellulose* **2015**, *22*, 935–969. **DOI:**10.1007/s10570-015-0551-0
51. S. A. Wahib, D. A. Da'na, M. A. Al-Ghouti, *Arab. J. Chem.* **2022**, *15*, 103650. **DOI:**10.1016/j.arabjc.2021.103650
52. A. J. Ali, A. Danladi, M. M. Bukhari, B. B. Nyakuma, *J. Nat. Fibers* **2020**, *19*, 2756–2771. **DOI:**10.1080/15440478.2020.1856279
53. S. Zarina, I. Ahmad, *BioRes.* **2015**, *10*, 256–271. https://bioresources.cnr.ncsu.edu-/resources/biodegradable-composite-films-based-on-k-carrageenan-reinforcedbycellu-losena-nocrystal-from-kenaf-fibers/
54. K. Benhamou. Extraction de nanofibrilles de cellulose à structure et propriétéscon-trôlées : caractérisation, propriétésrhéologiques et application nanocomposites, Gre-noble Alpes, Maroc, **2015**, 173- 240. https://theses.hal.science/tel-01260323

Povzetek

Celuloza je najbolj razširjen in obnovljiv polimer v naravi. Odlikuje ga biorazgradljivost, ki pomaga ustvarjati prijazno okolje. Ta študija želi opisati nanocelulozo, pridobljeno iz odpadkov datljeve palme, tako posušenih (DP) kot svežih palm (FP) z uporabo kemijskih metod (hidroliza s H_2SO_4). Fizikalne lastnosti, morfologijo, elementarno sestavo in termično stabilnost smo določili s Fourierjevo transformacijsko infrardečo spektroskopijo (FTIR), rentgensko difrakcijo (XRD), zeta sizerjem, vrstično elektronsko mikroskopijo (SEM) in energetsko disipativno rentgensko *analizo* (EDX) in termogravimetrično analizo (TGA). Rezultati FTIR, SEM in EDX so razkrili učinkovito odstranjevanje nečistot, hemiceluloze in lignina. Po obdelavi so vzorci posušene palme (DR) vsebovali 35,99% celuloze in 33,12% celuloznih nanokristalov (CNC), vzorci sveže palme (FP) pa 36,17% celuloze in 34,35% CNC. CNC ima večjo kristaliničnost kot surova vlakna in Zeta potencial je bil med 25 in 1150 nm. Analiza TGA je pokazala dobro toplotno odpornost DP.